

On the time-scale of thermal cycles associated with open-vent degassing

L. Spampinato · C. Oppenheimer · A. Cannata ·
P. Montalto · G. G. Salerno · S. Calvari

Received: 13 July 2011 / Accepted: 8 March 2012 / Published online: 1 April 2012
© Springer-Verlag 2012

Abstract Thermal imagery obtained with portable infrared cameras is widely used to track and measure volcanic phenomena. In the case of explosive eruptions, both air and ground-based thermal monitoring have enabled collection of data streams from relatively safe distances. Analysis of these data have enabled the characterisation of different explosive regimes, parameterisation of eruptive plumes, and assessment on the dynamics occurring in the shallow system. Here we explore the suitability of infrared imagers for investigating the short time scale eruptive behaviour of three basaltic volcanoes. We present high-time resolution thermal image data-sets recorded at Etna, Stromboli and Kīlauea volcano. At the time of observations, all three exhibited pulsed degassing. Signal processing of the mean apparent temperature time-series highlights four broad classes of cyclic temperature changes at the three volcanoes based on characteristic time-scales revealed in the periodograms: (1) <15 s, (2) ~20–50 s, (3) ~1–10 min, and (4) 12–90 min. Based on previous studies and integrating time-series results with qualitative visible and thermal observations and, in case of Kīlauea, also with SO₂ column amounts in the plume, we

hypothesise that short cycles relate mainly to bursting of overpressured gas bubbles at the magma surface, while long cycles might be associated with mechanisms of gas slug formation and ascent, and to the emplacement and drainage of a lava lake. At Kīlauea, slow fluctuations may reflect periodic variations of the lava lake surface level. The data from all three volcanoes reveal superimposition of degassing cycles of different frequencies, suggesting link through common magmatic processes and physical properties.

Keywords Thermal imaging · SO₂ DOAS measurements · Superimposed cycles · Basaltic volcanoes

Introduction

Volcanic degassing provides crucial information on the dynamics of magmatic systems and eruptions (e.g., Blake 1984; Dingwell 2001; Varley and Taran 2003). In the case of basaltic volcanoes, a variety of field and laboratory studies have led to models of degassing and explosive activity, and their correlation with magma transport within conduits and gas bubble nucleation, growth, coalescence and separation (e.g., Wilson 1980; Jaupart and Vergnolle 1988; Ripepe et al. 2001; James et al. 2004, 2006; Parfitt 2004). Commonly, experiments simulate low viscosity two-phase magmatic flows by analogue liquid–gas systems (e.g., Vergnolle and Jaupart 1986), thus neglecting the magma crystal content (e.g., Navon and Lyakhovsky 1998). Depending on the gas and liquid volume fractions in the mixture, Vergnolle and Mangan (2000) recognised four representative two-phase flow regimes: bubbly, slug, annular, and dispersed flow.

Strombolian eruptions, thought to correspond to a slug-flow regime, consist of discrete, rhythmic bursts of gas

Editorial responsibility: R. Cioni

L. Spampinato (✉) · A. Cannata · P. Montalto · G. G. Salerno ·
S. Calvari
Istituto Nazionale di Geofisica e Vulcanologia,
Osservatorio Etneo, sezione di Catania,
Catania, Piazza Roma, 2,
95123, Italy
e-mail: spampinato-l@ct.ingv.it

L. Spampinato · C. Oppenheimer · G. G. Salerno
Department of Geography, University of Cambridge,
Downing Place,
Cambridge CB2 3EN, UK

bubbles at the magma free surface, which hurl pyroclasts a few tens or hundreds of metres into the air (e.g., Blackburn et al. 1976; Sparks 1978; Wilson 1980; Vergnolle and Brandeis 1996). Gas-pistoning is a further expression of slug flows (e.g., Ripepe et al. 1993; Vergnolle and Mangan 2000), consisting of regular rise and fall of magma level within a volcanic conduit triggered by the ascent and release of large gas pockets. This kind of activity, extensively studied at Hawaiian volcanoes (e.g., Tilling 1987; Johnson et al. 2005), has also been associated with gas accumulation beneath the surface crust and its periodic failure and release (Swanson et al. 1979; Patrick et al. 2010). Additional degassing regimes recognised at open-vent basaltic systems include gas puffing, gas jetting, and churn-turbulent type flow regime. The former, commonly observed at Stromboli volcano, has been associated with the simultaneous bursting of large concentrations of small (~1 mm diameter) gas bubbles (Ripepe et al. 2002; Patrick 2007a; Patrick et al. 2007; Landi et al. 2011). Gas jetting involves the emission of high-temperature, high-pressure gas, usually accompanied by ash-lapilli pyroclasts (e.g., Calder et al. 2000; Ripepe et al. 2001; Palma et al. 2008). The churn-turbulent type flow regime occurs when gas flow rate is high, gas fraction exceeds 20 %, flow is turbulent, coalescence is pronounced, and large bubbles form (Xu et al. 1999; Mudde 2005; Palma et al. 2008).

The monitoring and study of degassing behaviour of volcanic systems, in terms of gas composition and regime, has been undertaken using direct sampling methods (e.g., Noguchi and Kamiya 1963; Symonds et al. 1996) and remote sensing techniques (e.g., Stoiber and Jepsen 1973; Realmuto et al. 1994; Oppenheimer et al. 1998; Salerno et al. 2009), including thermal imaging (e.g., Patrick 2007b; Spampinato et al. 2008a). The latter technique is increasingly used in volcano surveillance and monitoring (e.g., Francis 1979; Spampinato et al. 2011), as well as for modelling volcanic degassing (e.g., Oppenheimer et al. 2004, 2009; Harris and Ripepe 2007; Spampinato et al. 2008b; Patrick et al. 2011) and explosive styles (e.g., Patrick 2007a, b; Patrick et al. 2007). In particular, the study of thermal waveforms has allowed the discrimination and characterisation of different volcanic degassing styles. Harris et al. (2003), for instance, observed that time-series of (i) strombolian eruptions present thermal transients with impulsive onsets that correspond to the explosion, emission and passage of ballistics and gas components through the detector field-of-view; (ii) gas jetting is characterised by waveforms similar to those of the strombolian eruptions; and (iii) persistent degassing displays a persistent high thermal signal with overprinted oscillations relating to gas puffing.

In this paper, we investigate the capability of high-time resolution thermal data for the discrimination of cyclic patterns of the degassing regime at three open-vent basaltic

volcanoes: Etna (Italy), Stromboli (Italy), and Kīlauea (Hawai'i). In addition, for Kīlauea, high-time resolution SO₂ abundance measurements have been obtained. Integrating time-series analysis with visible and thermal observations of the simultaneous eruptive activity from the three volcanoes, we attempt to evaluate the significance of the recognised cyclic patterns in terms of magma transport, dynamics of degassing, and associated eruptive mechanisms and styles.

Field sites and prevailing activity

At Mount Etna, thermal images were collected in July 2006, during an eruption at the South-East summit crater (SEC), from a distance of ~450 m (Fig. 1a–c). The event started on 14 July 2006 on the south-eastern flank of the SEC. It was characterised by explosive activity of variable intensity from a cluster of vents aligned ESE-WNW at ~3150 m elevation, and by lava effusion ~145 m downslope (e.g., Neri et al. 2006; Salerno et al. 2009). The eruption lasted until 24 July. On the morning of 19 July, at the time of our measurements (from 08:26 to 09:37 local time; all times are local), the explosive activity consisted of jets of hot, bluish gases with minor content of pyroclasts, gas puffing, and spattering from three vents (V₁, V₂, and V₃ in Fig. 1c). Ballistic bombs and blocks spread radially around the cone rim reaching, and eventually burying, the downslope lava channel, forming tube-like structures (Fig. 1c). Puffs and explosions fed a strombolian-style activity with short intervals between events, and continuous emission of pressurised gas.

At Stromboli, the ground-based thermal survey was carried out on 4 September 2008 from 09:40 to 10:10, during a period of typical eruptive activity, involving four of the five vents then present within the summit crater terrace (Cristaldi 2008; Fig. 1d–f). The eruptive activity was vigorous, and associated with formation of cinder cones, hornitos, and pyroclastic deposits within the crater depression (Fig. 1e–f). Intermittent explosions took place at two vents in the north-eastern area of the crater terrace (vents ne₁ and ne₂), and from one of the two vents of the south-western zone (vent sw₂), while steady gas puffing was observed from the central zone (vent cc). The measurement distance was approximately 300 m.

At Kīlauea volcano, thermal data were recorded between 10:10 and 14:38 on 11 May 2008 following the opening of a vent on the southern wall of Halema'uma'u crater on 19 March 2008 (Wilson et al. 2008; Poland et al. 2009; Fee et al. 2010; Fig. 1g–i). The vent opened while the effusive activity from the East Rift was ongoing, with lava flowing via tubes to the coast and into the ocean, and magmatic degassing sustained through Pu'u 'Ō'ō crater (Poland et al. 2009; Fee et al. 2010). Our ground-based measurements focused on the new vent in Halema'uma'u crater and were

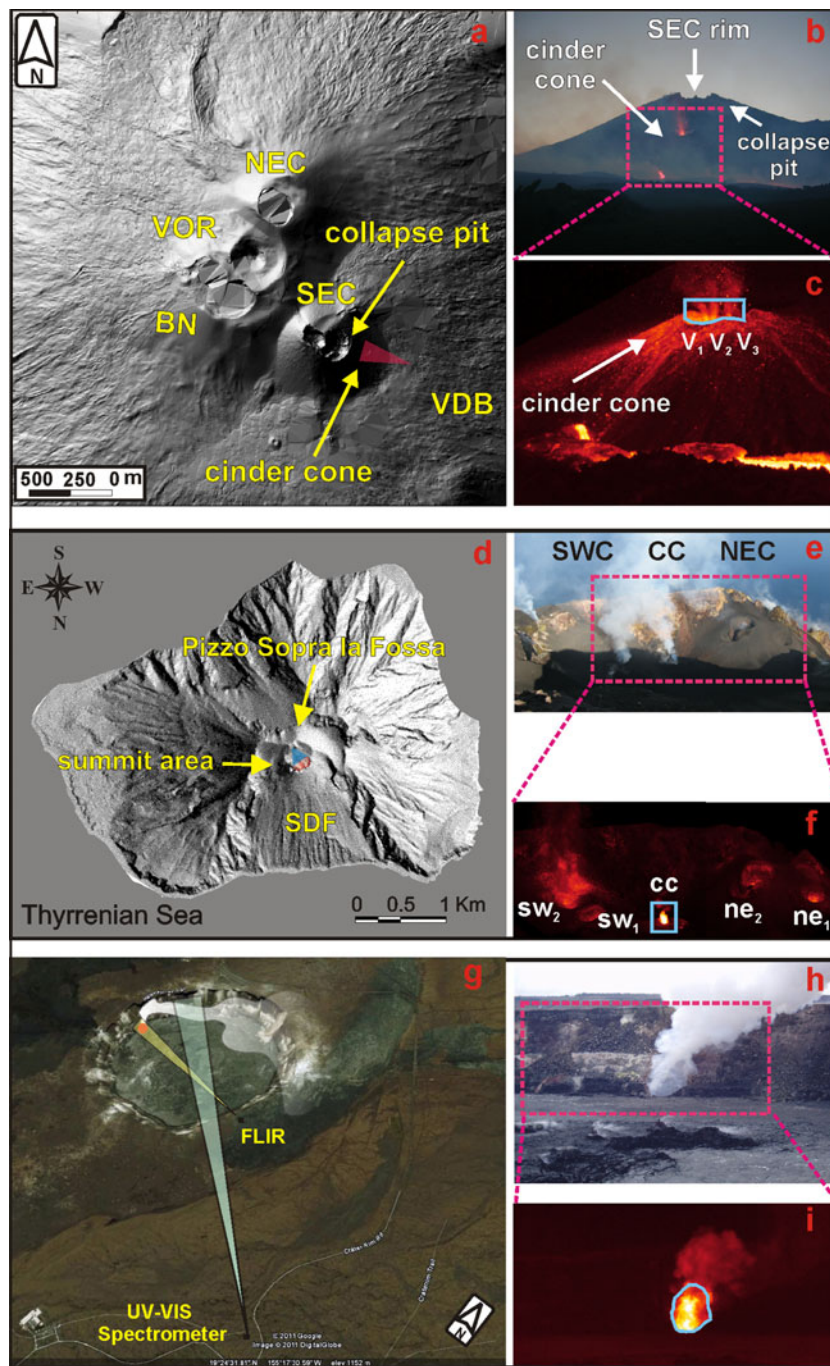


Fig. 1 Volcanoes and sites where thermal images were recorded: **(a)** shaded relief map of Mount Etna (Pareschi, INGV-Pisa) showing the four summit craters - North-East crater (NEC), Bocca Nuova (BN), Voragine (VOR), and South-East crater (SEC) - the Valle del Bove depression (VDB), the collapse pit that formed during the 2004–5 eruption on SEC eastern flank (Neri and Acocella 2006), and the July 2006 cinder cone that grew on the same side of the crater. The red triangle represents the thermal camera’s field-of-view (FOV). **(b)** and **(c)** are visible and thermal images showing the explosive vents (V_1 , V_2 , and V_3) and effusive activity, from the top and base of the July 2006 cinder cone, respectively. **(d)** shaded relief map of Stromboli volcano showing the summit area, the topographic high of Pizzo Sopra la

Fossa, and the Sciara del Fuoco depression (SDF). The blue triangle is the thermal camera’s FOV. **(e)** and **(f)** visible and thermal images of the crater terrace, respectively. SWC, CC, and NEC are the South-West crater, Central crater, and North-East crater, respectively. ne_1 , ne_2 , cc, sw_1 , and sw_2 are labels for the active vents. Note that for this study, we focused just on cc. **(g)** satellite image of Halema’uma’u crater (Google Earth) with the site of the vent (red dot) that opened on 19 March 2008 and the FOV of the thermal camera (in yellow) and of the ultraviolet–visible (UV–VIS) spectrometer (in light green). **(h)** and **(i)** visible and thermal images of the vent, respectively. The cyan contours in **(c)**, **(f)**, and **(i)** enclose the regions of interest investigated in each of the three case study volcanoes by thermal imagery

made at a distance of 700 m. At this time, we observed strong degassing producing a whitish plume that was bent over by the wind as soon as it reached the crater rim. Near the vent, the plume was transparent, bluish and turbulent.

During the fieldwork at Kīlauea, we also collected SO₂ data within the same time period of thermal imagery. In detail, two data-sets were collected of which the first was recorded between 10:47 and 11:47 and the second from 12:16 to 13:36.

Methods: data collection and time-series analysis

Thermal images were collected using PM695 (at Etna and Kīlauea) and P640 (at Stromboli) thermal cameras manufactured by FLIR Systems. Both models consist of uncooled microbolometers equipped with 320×240 (PM 695) and 640×480 (P640) focal plane arrays, and sensitive in the 8–14 μm waveband. Both instruments have a 24°×18° field-of-view (FOV). Thermal images were acquired at rates of 1, 2, and 15 frames per second at Etna, Kīlauea, and Stromboli, respectively. Air temperature and relative humidity, and path lengths were recorded for subsequent atmospheric correction of the measured radiance (Spampinato et al. 2011). Following previous studies, emissivity was set to 0.99, 0.95, and 0.96 at Etna, Stromboli and Kīlauea, respectively (e.g., Calvari et al. 2005; Spampinato 2008; Spampinato et al. 2008a). Comparison of the recorded ambient air relative humidity and temperature with the thermal data (e.g., Chiodini et al. 2007; Spampinato et al. 2011), confirmed that the observed trends in temperatures in the imagery were not due to atmospheric variability. Based on the line-of-sight distances at the three sites and the instantaneous FOVs of the two instruments, we estimated a nominal pixel dimension corresponding to 0.62, 0.21, and 0.98 m at Etna, Stromboli, and Kīlauea, respectively. Photographs were also captured during data acquisition to aid subsequent interpretation.

From thermal images recorded at the three volcanoes, we derived time-series of the mean apparent temperatures (Fig. 2) extracted from regions of interest (ROI; cyan contours in Fig. 1c, f, i) of the hottest parts of the volcanic plumes of Etna (ROI area ~230 m²), Stromboli (ROI area ~77 m²), and Kīlauea (ROI area ~790 m²), very close to the vent areas. Given that our aim was to identify time variations in thermal signals rather than retrieve robust radiometric values, and that all data were collected with fixed viewing positions, we did not geometrically correct the imagery (Ball and Pinkerton 2006; Spampinato et al. 2011).

At Kīlauea, SO₂ data were collected (pink shading in Fig. 2c), using an ultraviolet spectrometer and scattered sunlight as the light source. The two data-sets were collected using an Ocean Optics USB2000 spectrometer with spectral

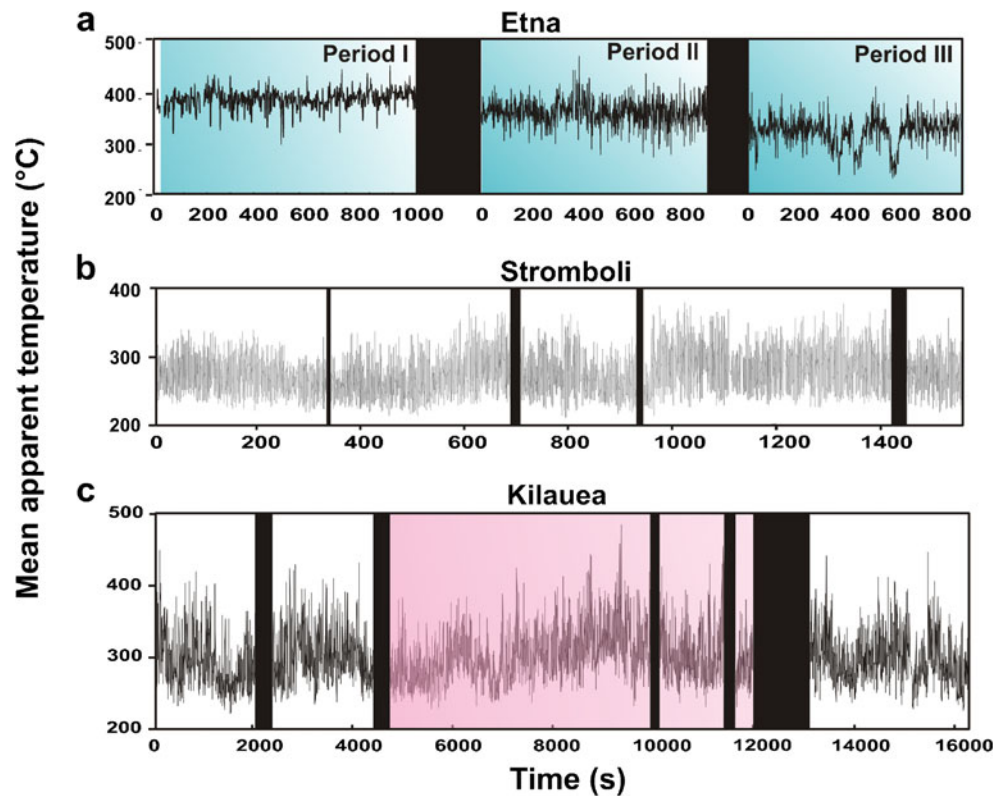
range of 295–375 nm and ~0.44 nm FWHM spectral resolution. Individual spectra were collected from the north-west side of the caldera, ~2 km from the plume (Fig. 1c), with a time step of 17 s. Spectra were evaluated using the WinDoas software package (Fayt and Van Roozendaal 2001) applying the standard Differential Optical Absorption Spectroscopy (DOAS) technique (Platt and Stutz 2008), and fitting of the 305–316 nm spectral window to yield time-series of the column amounts (CA) of SO₂ in the FOV of the spectrometer. We consider these to provide, to first order, a proxy for SO₂ flux, as observations elsewhere (e.g., Boichu et al. 2010) have shown that during gas puffing, both plume velocity and column amounts increase.

The nature of the long and short scale fluctuations within both thermal and SO₂ CA time-series was investigated using two time-series analysis techniques. The first was the Fourier Transform analysis (application of the Fast Fourier Transform, FFT) that provides information on the signal power content at any frequency but loses the frequency location in the time domain. This widely used technique is designed for stationary signals; however, many geophysical signals, such as ours, contain non-stationary or transitory characteristics: drift, trends, abrupt changes, and onsets and ends of events. These characteristics are often the most important part of the signal, and Fourier analysis is not suited for their detection. For this reason, we also applied the Wavelet Transform (WT; e.g., Cazelles et al. 2007; Spampinato et al. 2008b). In contrast to the Fourier transform, which consists of a linear superposition of independent and non-evolving periodicities, the WT is based on the convolution of signals with a set of functions derived from the translations and dilatations of a basic function called the “mother wavelet”. Thanks to these features, the WT preserves frequency location in the time domain, and by use of variably-sized cells we could identify time location of both the low- and high-frequency features in our time-series (Daubechies 1990; Bartosch and Seidl 1999; Grinsted et al. 2004; Patanè et al. 2007).

Results

At Mount Etna, mean apparent temperatures of the ROI (Fig. 1c) were derived from a ~60 min-survey (Period I, II, and III in Fig. 2a). The retrieved time-series contain wide-band spectra of low- and high-frequency components with temperatures ranging from ~230 to 470°C. The general behaviour shows an increasing initial trend from ~360 to 410°C (Period I), followed by a gradual decrease to 330°C (Periods II and III), with in Period III (350–700 s) three sharp minima of 247, 242, and 230°C at 400, 500, and 650 s, respectively. For Stromboli, we gathered ~25 min of imagery for vent cc, from which the extracted mean

Fig. 2 Variability of the mean apparent temperature within the ROI of (a) 19 July 2006 at Mount Etna's SEC, (b) 4 September 2008 at Stromboli's cc vent, and (c) 11 May 2008 at Halema'uma'u crater vent. The black regions indicate missing data. The pink region in (c) shows the time window during which SO₂ measurements were carried out



apparent temperatures show a roughly sinusoidal trend between ~ 200 and 370°C (Fig. 2b). As in the previous case, the time-series is characterised by both long wavelength and rapid fluctuations. On 11 May 2008, at Halema'uma'u crater, we recorded thermal images for more than 4 h (Fig. 2c). The main trend of the mean apparent temperatures is marked by several irregular fluctuations (between ~ 220 and 480°C).

Figure 3a, b, and c represent the power spectra and statistical significance computed by FFT according to the hypothesis of background red noise (Torrence and Compo 1998), which considers reliable only the peaks lying above the 95 % confidence limit (the green dashed lines in Fig. 3). The power spectra for the Etna time-series exhibit similar long periods of 1–10 min (Period I) and 1–5 min (Periods II and III), and significant short periods of 45, 9 and 5 s (Period I), 23 and 4 s, and 7 and 5 s (Period II and III; Fig. 3a). In the case of Stromboli, the power spectral analysis of the mean apparent temperatures (Fig. 2b) highlights long periods of 5–8 min and short periods of ~ 1 –2 s (Fig. 3b). Kilauea's mean apparent temperatures (Fig. 2c) display significant peaks at 12–90 and 3–8 min, 42–48 s, and < 15 s (Fig. 3c).

The results obtained by power spectral analysis are consistent with those obtained by WT (Fig. 4a, b, and c), and show significant spectral power (highlighted by the black line at 95 % confidence interval), that for Etna are mainly between ~ 128 –256 s (~ 2 –4 min) and ~ 64 –256 s (~ 1 –4 min) for Period I, and II and III, respectively (Fig. 4a). In

addition, in Period I and II, periodicities ranging between a few seconds and ~ 64 s (~ 1 min) are observed (Fig. 4a). For Stromboli, we have found periodicities between ~ 120 –540 s (~ 2 –9 min) and 1–2 s (Fig. 4b), and for Kilauea between ~ 510 –5400 s (~ 8 min - 1.5 h), ~ 128 –512 s (~ 2 –8 min), 30–60 s (30 s - 1 min), and minor spectral components below 15 s (Fig. 4c). Additionally in the three case studies, the WT showed that some of the identified periodicities were stationary features of the analysed time-series, whereas others seemed to be not steady but localised in time. In particular, for Stromboli the periodicities ~ 120 –540 s were evident in the middle of the analysed time window, while the 1–2 s cycles appeared as a stationary feature. For Kilauea the periodicities ~ 510 –5400 s were present in the whole time-series, whereas the higher frequency components (below 15 s) were well localised in specific time intervals.

On 11 May 2008, at Halema'uma'u crater, the SO₂ CA ranged between 2 –7 and 1 – 7×10^7 molecules cm^{-2} , in the first and second data-set, respectively (Fig. 5a and b). The first time-series (Fig. 5a) has a mean value of 4×10^7 molecules cm^{-2} and is characterised by wide fluctuations. The second (Fig. 5b), marked by rapid variations, displays mean values of 2×10^7 molecules cm^{-2} , a factor of 2 less than Fig. 5a. To compare the two time-series with thermal data, we have analysed the SO₂ CA emission pattern applying the FFT (Fig. 5c and d) and the WT (Fig. 5e and f). Both methods highlighted significant periods of 8 and 1 min and 48 s in Fig. 5c, and e, and 26, 15, and 1 min in

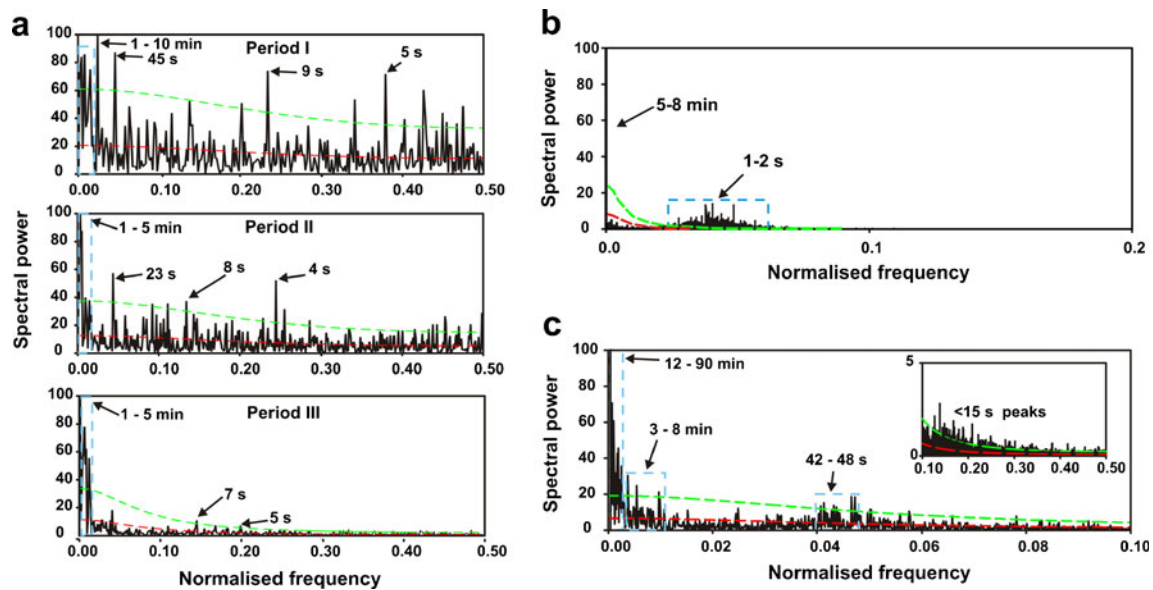


Fig. 3 Power spectra and statistical significance computed by Fast Fourier transform according to the hypothesis of background red noise (Torrence and Compo 1998) for Etna (a), Stromboli (b), and Halema'uma'u crater (c) using the thermal data shown in Fig. 2

Fig. 5d and f, with WT analysis providing time location of the observed periodicities.

Discussion of identified cycles

Numerous studies have identified cycles in the degassing (chemical composition, flux, and temperature) of a variety of magmas, including basaltic (e.g., Oppenheimer et al.

2004; Harris and Ripepe 2007; Spampinato et al. 2008b) and phonolitic (Oppenheimer et al. 2009; Boichu et al. 2010). The starting point for interpretation of the cyclic behaviour we identify here is that the variations reflect magmatic processes - we discount any effects of atmospheric turbulence because of the high magmatic temperatures recorded and their association with observed magmatic activity at the three volcanoes. The next consideration is whether the cycles result from pulses or episodic behaviour

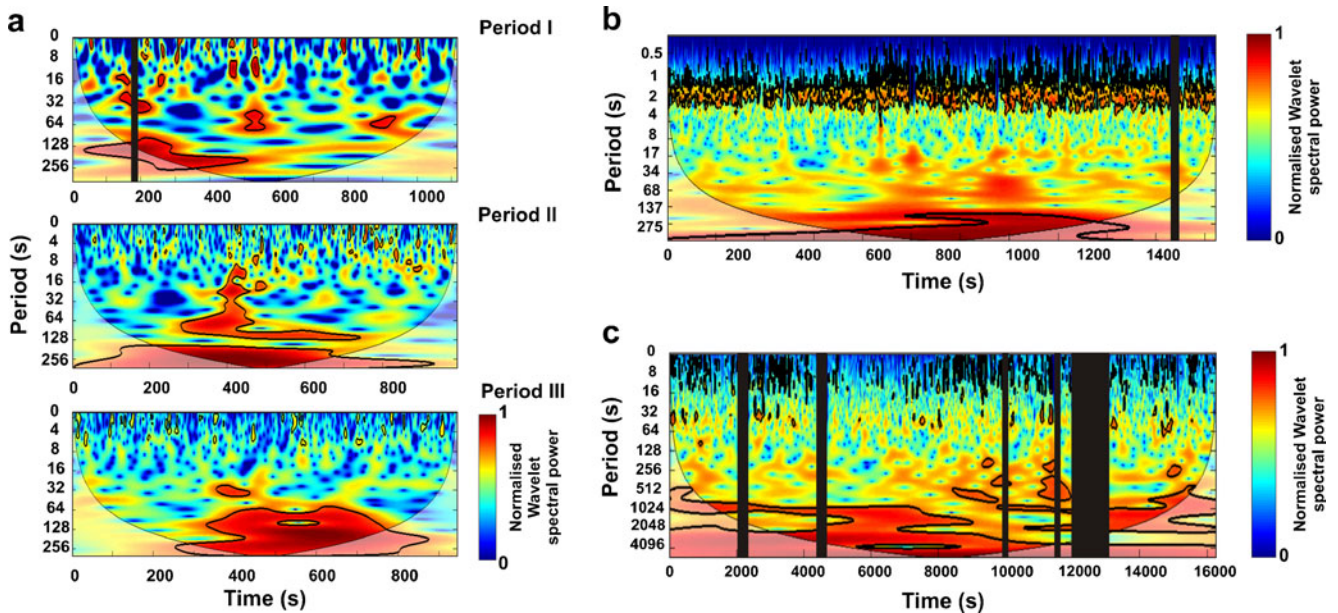


Fig. 4 Wavelet transform computed by Matlab toolbox provided by Grinsted et al. (2004) applied to the thermal data shown in Fig. 2 for (a) Etna, (b) Stromboli, and (c) Halema'uma'u crater. The solid contour shows the 95 % confidence interval and the light shaded region the

cone of influence, the area where the wavelet spectrum is affected by edge effects (Torrence and Compo 1998). The black bands indicate missing data

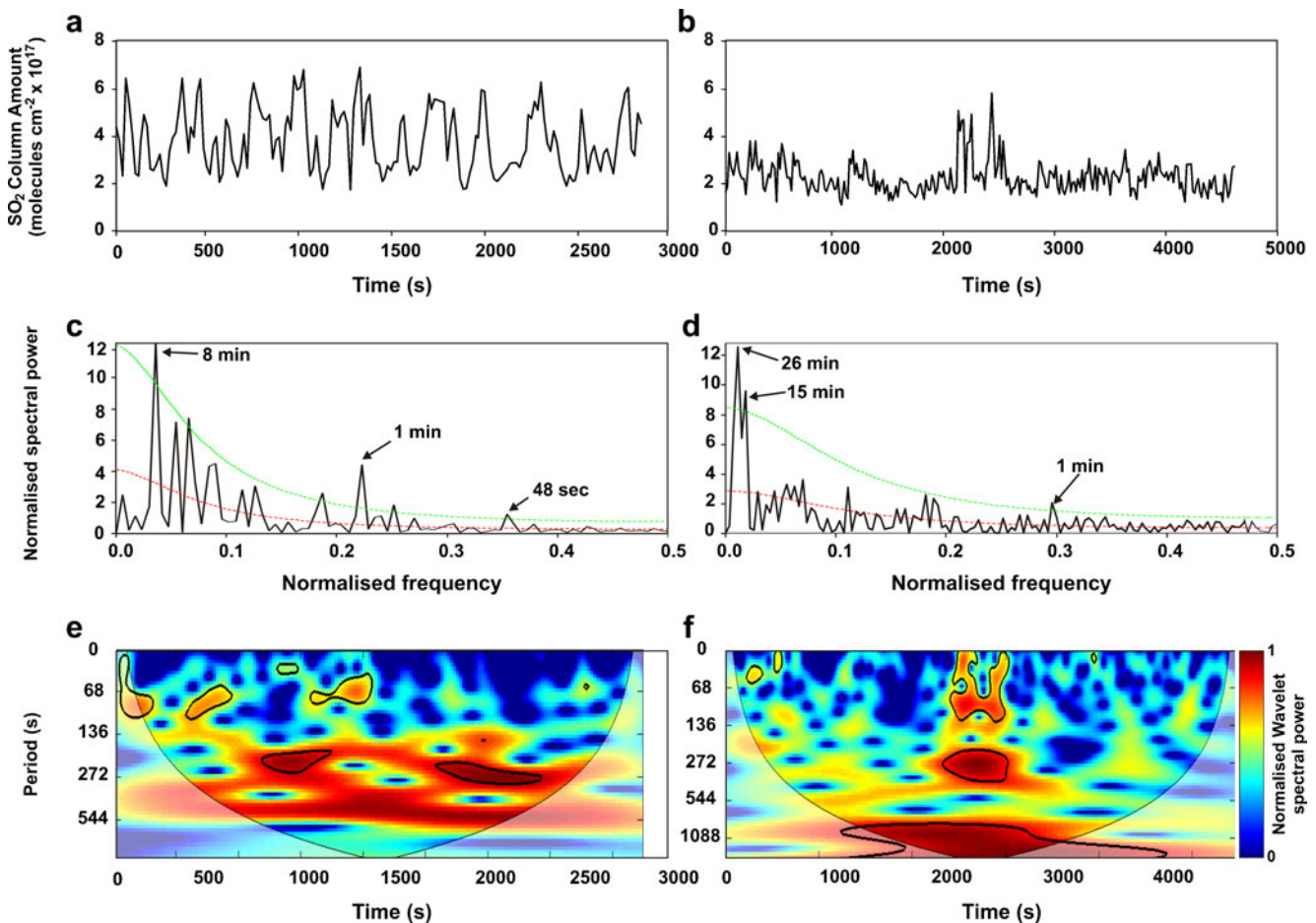


Fig. 5 (a) and (b) time-series of the SO₂ column amounts retrieved for data collected at Halema'uma'u crater on 11 May 2008. (c) and (d) are the corresponding power spectra and statistical significance computed by Fast Fourier transform. (e) and (f) Wavelet transform applied to (a)

and (b). As for Fig. 4, the solid contour shows the 95 % confidence interval and the light shaded area the cone of influence (Torrence and Compo 1998)

- i.e., that they are more or less discrete events superimposed on background behaviour (like strombolian eruptions every 10 min), or are a waxing and waning phenomenon with a more continuous time response. The latter might result, for instance, from oscillations in magma flow reflecting flow instabilities that develop in the shallow region of the conduit (e.g., Burton et al. 2007; Oppenheimer et al. 2009), or from gas segregation processes that accumulate and release bubbles continuously rather than as discrete foam collapse events (e.g., Blackburn et al. 1976).

Inspection of the time-series analyses presented here, combined with observation of the eruptive activity at the surface, yields insights into the origins of the identified cyclic behaviour.

Mount Etna

Time-series analysis of the observations for Mount Etna identified periods of 4–9 s, 23–45 s, and 1–10 min. Based on visual observations of the prevailing activity, we can

attribute the 4–9 s cycles (Figs. 3a and 4a) to gas puffing and/or discrete, mostly type 1-like strombolian explosions (Patrick et al. 2007) at vents V₁, V₂ and V₃ (Figs. 1c, 3a and 4a). The longer periodic behaviour corresponding to 23–45 s and 1–10 min cycles relate to the occurrence and duration of strombolian eruptions. Each of these eruptions includes emission of a hot, overpressured gas jet (Calder et al. 2000) at the beginning (thus every 23–45 s or 1–10 min), followed by a sequence of discrete strombolian bursts at 4–9 s intervals.

The occurrence of these multiple cycles is explicable if we consider that strombolian eruptions not only exhibit a wide spectrum of eruptive styles (e.g., Patrick et al. 2007), but can also result from bursting of either single large overpressured gas bubbles or clusters of bubbles (e.g., Blackburn et al. 1976; James et al. 2004, 2006). If this is the case, then we suggest the 23–45 s and 1–10 min cycles represent clusters of bubbles approaching the surface, inducing sequences of events with short intermissions. As in the case of single gas slugs, clusters of bubbles require a phase of

bubble stacking and coalescence either as they ascend in the conduit or following accumulation in asperities of the plumbing system (e.g., Jaupart and Vergnolle 1988; Ripepe and Gordeev 1999; Vergnolle and Mangan 2000; Menand et al. 2003).

Assuming that the geometry of the SEC conduit/dike was stabilised during our observations, and bearing in mind that a few hours after our survey, the activity evolved from the weak phase of Period III to a pure lava effusion and then to intense lava fountaining (by ~18:00), then the decrease in mean apparent temperature from Period I to III might reflect gradual reduction of the degassing efficiency within the shallow feeding system, probably due to gas stacking and accumulation prior to the lava fountaining episode of the late evening (Vergnolle and Ripepe 2008). Following Allard et al. (2005), Spilliaert et al. (2006) and Bonaccorso et al. (2011), gas accumulation and foam development occur at depths of ~1.5–1.8 km below SEC. If we consider also the phase of gas bubble accumulation, foam development and collapse (e.g., Jaupart and Vergnolle 1988, 1989), the overall cyclic pattern that we have here recognised might represent short-term eruptive signals superimposed on long-term eruptive processes, i.e. the accumulation and collapse of gas bubble foam leading transition from strombolian explosions to lava fountains (e.g., Vergnolle and Ripepe 2008). In this context, we speculate that the decrease in duration of the strombolian eruptive cycles from Period I to Periods II and III might reflect a gradual waning of the degassing process within the volcano's shallow feeding system. Period I strombolian cycles lasted between 1–10 min with respect to the 1–5 min of both Periods II and III, suggesting stronger gas supply, and hence higher degassing efficiency, with respect to the following Periods II and III. Visually, these latter periods were characterised by slow waning of the explosive activity, characterised by low energy discrete explosions when compared to those of Period I.

Stromboli Volcano

At Stromboli, we identified two distinct cycles, one on the order of a few seconds and the other on the order of minutes (Figs. 3b and 4b). Short periods of 1–2 s are consistent with the sustained, high-frequency release of gas pockets at the surface, known as gas puffing. These short cycles have been previously detected at Stromboli by thermal and acoustic techniques (Ripepe et al. 2002). Gas puffing relates to a persistent overpressured bubbly flow regime that, at Stromboli, is generally stable at a single crater but can shift from one crater to another (e.g., Ripepe et al. 2002, 2008; Harris and Ripepe 2007; Landi et al. 2011). This mode develops when gas is regularly released in discrete bursts or puffs occurring every few seconds, each triggered by the ascent of discrete bubble bands or layers (Ripepe et al. 1996; Ripepe

and Gordeev 1999; James et al. 2004). These might result from a number of factors including steady volatile exsolution due to differential gas bubble velocity producing flow instability waves in magma (Manga 1996), spontaneous variations in the coalescence of a foam that had developed at the roof of a shallow reservoir (e.g., Jaupart and Vergnolle 1989), and rising of gas-rich magma in discrete pulses within the volcano upper feeding system (Ripepe et al. 2002). In detail, in the first case, the large concentration of small bubbles increases the local viscosity of magma allowing bubbles to ascend in bands of bubble populations, with single bubbles rising faster than the bands, bursting with frequencies of a few seconds (Ripepe et al. 2002).

Puffing can occur in either of two regimes: vigorous and weak (Ripepe et al. 2002). Ripepe et al. (2002) related the variability of this degassing mode to changes in magma supply and band rise rates. Additionally, these authors showed that the two regimes alternated every ~5–40 min, and that the vigorous phase was characterised by 1–2 s puff periodicity, whereas the weak phase by periods of ~3–5 s.

Although the relatively short duration of our data-set, we could clearly recognise the kind of puffing regime occurring during our survey, i.e. the 1–2 s vigorous regime observed by Ripepe et al. (2002). Moreover, we have found a 5–8 min cycle that is in between the frequencies typical of gas puffing and the 5–40 min duration of each of the puffing regimes (Ripepe et al. 2002). This cycle might represent minor fluctuations within the vigorous puffing regime, and is visually associated with gradual increases/decreases of puff size and waxing and waning vent glow that might result from changes in magma level within the vent.

Kīlauea Volcano

At Halema'uma'u crater, we have related periodicities <15 s to rapid pulsing of the volcanic plume characterised by sharp increases in the mean apparent temperatures, reminiscent of gas puffing at Stromboli and Etna (Ripepe et al. 2002; Lautze et al. 2004). Fee et al. (2010) found that nearly all of the degassing bursts at Halema'uma'u generate infrasound in the long period (LP) band (~1–10 s, i.e., 0.1–1 Hz), while only a few have very-long period (VLP) components (~10–33 s, i.e., 0.3–0.1 Hz). The authors attributed the source of the infrasound to unsteady degassing of magma into a stationary gas-filled volume cavity (volume of $\sim 3 \times 10^6 \text{ m}^3$ in November 2008) beneath the vent (at depth of ~219 m in November 2008) that is excited into resonance. Patrick et al. (2011) observed that the summit activity generated significant VLP seismic signals (1 km depth source; Chouet and Dawson 2008) associated with degassing from the top of a lava column. In particular, Patrick et al. (2011) proposed that VLP seismic signals reflected rapid

transmission of forces, sourced at the top of the magma column, to the 1 km depth coupling location.

Periods of 42–48 s in the thermal data are consistent with the 48 s - 1 min cycle found in the simultaneous collected SO₂ CA time-series, and reflect thermal and degassing fluctuations that might result from the bursting of gas bubbles releasing hot gas at the surface. This activity is consistent with the cycles of spattering observed during a helicopter-borne survey performed in early September 2008, which revealed a lava lake within the Halema`uma`u crater vent (Patrick et al. 2008). The lake surface was characterised by moderate bubbling, followed by several minutes of vigorous spattering. This led us to propose that the eruptive activity reflected a gas piston-like mechanism. Gas pistoning describes the typical regime of degassing seen at several of Kīlauea's eruptive vents, and has been interpreted in contrasting models. According to Swanson et al. (1979) gas pistoning is driven by gas accumulation beneath a surface crust, which periodically fails releasing the shallowly accumulated gas. The second model is that of Vergnolle and Jaupart (1990), which defines gas pistoning as a phenomenon related to the periodic ascent of gas pockets (slug-type two phase flow) bursting at the surface. By multidisciplinary studies of the activity, Patrick et al. (2010) showed that gas pistoning of late 2010 was clearly associated with the gas accumulation model of Swanson et al. (1979).

Our considerations are consistent with the findings of Johnson et al. (2005), who observed similar periodicities (2–7 min cycles) in 2002 using infrared thermometers while studying gas pistoning at Pu`u `Ō`ō crater. The authors suggested that gas pistoning occurs when a stagnant cap of degassed magma develops in the conduit, forcing ascending gas bubbles to collect beneath. Depending on the shallow conduit and vent geometry, Johnson et al. (2005) defined three types of pistoning. The first is the classical lava pond gas pistoning identified by Swanson et al. (1979). The second consists of gas pistoning from a hornito-like structure with associated lava effusion; and the third type occurs when the ascending gas slug buoyancy pushes the cap upward until it eventually spreads out laterally within a subsurface cavity. Unloading of the conduit magma ends with explosive gas release, and lava drain-back. During our survey, there was no lava effusion at the vent, and we believe that the observed pulsatory variations in temperature and SO₂ abundance could have been triggered by either the first or third of these modes of pistoning, but most likely the first. Based on infrasonic and seismic data, Fee et al. (2010) and Patrick et al. (2011) suggested the presence of a vent cavity extending vertically above the lava column. Moreover, the vent was ~35 m wide and no juvenile material was found after the burst. This led Houghton et al. (2008) to propose that the initial degassing burst within the

Halema`uma`u crater might be either gas-driven or to have occurred at depth. The latter hypothesis implied that lava did not reach the free surface due to geometrical constrictions, i.e. the presence of a cavity.

An overall view of periodicities found in both thermal and SO₂ time-series suggest that, as observed by Patrick et al. (2008, 2011), the filling phase of the lake was associated with vigorous degassing in the form of lava bubbling at the surface. This was followed by the waning of lava lake activity, and formation of a surface crust leading to a gradual decrease in detected thermal radiance and SO₂ release. According to infrasound, tremor, and visual observations (Fig. 2 in Patrick et al. 2011), the lava lake rise phase was characterised by a reduction in degassing due to gas accumulation beneath the lava viscous skin. However, as soon as lava was at its high stand, gas release occurred rapidly inducing vigorous spattering (Patrick et al. 2010, 2011). The heat and gas losses resulted in increased magma density causing lava to drain back (e.g., Harris 2008), accompanied by increased spattering (Patrick et al. 2008, 2011). Patrick et al. (2011) reported that lava level descended every ~6 min, consistent with the 3–8 min cycles we observe in the thermal measurements and in the SO₂ column amounts.

Additionally, for Kīlauea, where we collected the longest time-series, we have also recognised a very long cycle of 12–90 min (Figs. 3c and 4c). In Fig. 2c, it corresponds to the longest fluctuations, which describe slow cycles of gradual increases and decreases of the mean temperature of the emitted gas. Owing to the SO₂ sampling rate and to the shorter duration of the time-series, we only retrieved SO₂ cycles of 15–26 min, however these are compatible to the 12–90 min thermal oscillations. The SO₂ time-series are, in fact, included within the slow temperature fluctuation of ~90 min of Fig. 2c (pink shading). Similar periodicities of 10–80 min were previously observed at Pu`u `Ō`ō crater lava pond in seismic and ground deformation data (Baker et al. 2003). Consistent with the observations and models of Patrick et al. (2011) and Johnson et al. (2005), we believe that these long fluctuations might correspond to the episodic seismic tremor source discussed by Patrick et al. (2011). The authors recognised two types of volcanic tremor: episodic tremor lasting ~30 min and consisting of a few minute-long spindle-shaped high amplitude bursts, and a steady tremor characterised by a roughly constant amplitude with no regular fluctuations.

Conclusions

The rhythmic and repeated events and their duration provide indications for tracking and constraining the associated physical mechanisms and their effects at the surface. The results obtained by time-frequency analysis applied to data-

sets recorded at Mount Etna, Stromboli, and Kīlauea, and previously at Erta 'Ale (Spampinato et al. 2008b) and at Erebus phonolitic lava lakes (Oppenheimer et al. 2009; Boichu et al. 2010), characterise volcanic features and reveal discrete cycles of magma/degassing dynamics, even when they were not evident from the time-series trend (e.g., the Mount Etna case). Time-series analysis of the mean apparent temperatures of the three volcano and SO₂ column amounts, in the case of Kīlauea, identifies four broad classes of periodicity (eruptive cycles), from a few seconds to hours, characterised by a distinct anomaly within the periodograms. In future, we suggest progress could be made by better integration of thermal, gas, infrasonic and seismic data-sets. Nevertheless, the similarities shown by Etna and Kīlauea and their comparison with other volcanoes are suggestive of analogous degassing processes. In the case of Stromboli, we identified cycles associated with a puffing regime that varies according to changes in gas supply.

The cycles retrieved for the three volcanoes vary within similar time windows, and thus can be grouped into three main classes: (i) cycles with periods <15 s related to sharp pulses in the thermal signal (gas puff/discrete strombolian explosions; Harris et al. 2003), (ii) periods between ~20–50 s and 1–10 min characterising both the thermal and SO₂ time-series and associated with bursting of hot, overpressured gas bubbles/trains of bubbles (Blackburn et al. 1976) at the magma-air interface, and (iii) long cycles with periods of 12–90 min reflecting dynamics occurring within the shallow magma supply system.

Our high-time resolution data-sets encourage further use of time-frequency analysis using longer time-series of observations such as those recorded by permanent networks, and their comparison and integration with geophysical parameters. This will enable discrimination of eruptive mechanisms, and the tracking of long-term eruptive cycles likely related to deeper sources crucial for forecasting the behaviour of steady-state volcanic systems.

Acknowledgements We thank J. Kauhikaua Scientist-in-Charge of the Hawaiian Volcano Observatory (HVO) and the HVO scientists for their support during our field campaign. We are indebted to M.R. Patrick, J. Sutton, and T. Elias for sharing observations and data. We are also grateful with A. La Spina for fruitful discussions. LS, GGS and CO thank the UK NERC for an urgency grant to carry out the field-work on Hawai'i (PI: M. Edmonds). CO also thanks the NERC for funding through the UK National Centre for Earth Observation (Theme 6 "Dynamic Earth and Geohazards", PI: B. Parsons). GGS acknowledges NOVAC EU-funded Sixth Framework Programme project 18354. The thermal survey carried out at Stromboli by SC was part of the 2007–09 INGV-DPC Project V2 "Paroxysm". This work has also benefitted from comments on an earlier version of the manuscript by W.G. Rees and H. Pinkerton. We thank R. Wright, M.R. Patrick, and the BV Editor R. Cioni for their useful and constructive reviews. LS thanks A.J.L. Harris for fruitful suggestions on an early version of the manuscript.

References

- Allard P, Burton M, Muré F (2005) Spectroscopic evidence for a lava fountain driven by previously accumulated magmatic gas. *Letters to Nature* 433:407–410
- Baker SR, Sherrod DR, Lisowski M, Heliker C, Nakata JS (2003) Correlation between lava-pond drainback, seismicity, and ground deformation at Pu'u 'Ō'ō. In: Heliker C, Swanson DA, Takahashi TJ (eds) *The Pu'u 'Ō'ō - Kūpaianaha eruption of Kīlauea volcano, Hawai'i: The first 20 years*. US Geol Surv Prof Pap 1676:53–62
- Ball M, Pinkerton H (2006) Factors affecting the accuracy of thermal imaging cameras in volcanology. *J Geophys Res* 111:B11203. doi:10.1029/2005JB003829
- Bartosch T, Seidl D (1999) Spectrogram analysis of selected tremor signals using Short-Time Fourier Transform and Continuous Wavelet Transform. *Ann Geofis* 42(3):497–506
- Blackburn EA, Wilson L, Sparks RSJ (1976) Mechanisms and dynamics of strombolian activity. *J Geol Soc Lond* 132:429–440
- Blake S (1984) Volatile oversaturation during evolution of silicic magma chambers as a trigger for an eruption. *J Geophys Res* 89:8237–8244
- Boichu M, Oppenheimer C, Tsanev VI, Kyle PR (2010) High temporal resolution SO₂ flux measurements at Mt. Erebus, Antarctica. *J Volcanol Geotherm Res* 190:325–336
- Bonaccorso A, Bonforte A, Calvari S, Del Negro C, Di Grazia G, Ganci G, Neri M, Vicari A, Boschi E (2011) The initial phases of the 2008–2009 Mt. Etna eruption: a multi-disciplinary approach for hazard assessment. *J Geophys Res* 116:B03203. doi:10.1029/2010JB007906
- Burton MR, Mader HM, Polacci M (2007) The role of gas percolation in quiescent degassing of persistently active basaltic volcanoes. *Earth Planet Sci Lett* 264:46–60
- Calder ES, Harris A, Peña P, Flynn L, Pilger E, Fuentealba G (2000) Combined thermal and seismic analyses of the Villarrica Lava Lake. In: *Congreso Geológico Chileno 9 Actas Ext Abs* 2:11–14
- Calvari S, Spampinato L, Lodato L, Harris AJL, Patrick M, Dehn J, Burton MR, Andronico D (2005) Chronology and complex volcanic processes during the 2002–2003 flank eruption at Stromboli volcano (Italy) reconstructed from direct observations and surveys with a handheld thermal camera. *J Geophys Res* 110:B02201. doi:10.1029/2004JB003129
- Cazelles B, Chavez M, De Magny GC, Guegan JF, Hales S (2007) Time-dependent spectral analysis of epidemiological time-series with wavelets. *J Royal Soc Interface* 4:625–636
- Chiodini G, Vilardo G, Augusti V, Granieri D, Caliro S, Minopoli C (2007) Thermal monitoring of hydrothermal activity by permanent infrared automatic stations: Results obtained at Solfatara di Pozzuoli, Campi Flegrei (Italy). *J Geophys Res* 112:B12206. doi:10.1029/2007JB005140
- Chouet B, Dawson P (2008) Source mechanism of explosive degassing at Kīlauea volcano imaged from inversion of very long period seismic waveforms. *EOS Trans Am Geophys Union* 89(53), Fall Meet Suppl V34A0-1
- Cristaldi A (2008) Rapporto settimanale sull'attività eruttiva dello Stromboli ripresa dalle telecamere di sorveglianza, 01–07 settembre 2008. INGV-Open file report Prot Int N UFGV2008/089.
- Daubechies I (1990) The Wavelet Transform time frequency localization and signal analysis. *IEEE Trans Inf Theory* 36:961–1004. doi:10.1109/18.57199
- Dingwell DB (2001) Magma degassing and fragmentation: Recent experimental advances. In: Freundt A, Rosi M (eds) *From magma to tephra*. Elsevier, pp 1–23
- Fayt C, Van Roozendaal M (2001) WinDOAS 2.1-Software User Manual. Belgisch Instituut voor Ruimte-Aeronomie Instituut d'Aéronomie Spatiale de Belgique, Brussels, Belgium

- Fee D, Garcés M, Patrick M, Chouet B, Dawson P, Swanson D (2010) Infrasonic harmonic tremor and degassing bursts from Halema'uma'u crater, Kīlauea Volcano, Hawai'i. *J Geophys Res* 115:B11316. doi:10.1029/2010JB007642
- Francis PW (1979) Infra-red techniques for volcano monitoring and prediction – a review. *J Geol Soc Lond* 136:355–359
- Grinsted A, Moore JC, Jevrejeva S (2004) Application of the cross wavelet transform and wavelet coherence to geophysical time series. *Nonlinear Proc Geophys* 11:561–566
- Harris AJL (2008) Modeling lava lake heat loss, rheology, and convection. *Geophys Res Lett* 35:L07303. doi:10.1029/2008GL033190
- Harris AJL, Ripepe M (2007) Temperature and dynamics of degassing at Stromboli. *J Geophys Res* 112:B03205. doi:10.1029/2006JB004393
- Harris AJL, Johnson J, Horton K, Garbeil H, Ramm H, Pilger E, Flynn L, Mouginiis-Mark P, Pirie D, Donegan S, Rothery D, Ripepe M, Marchetti E (2003) Ground-based infrared monitoring provides new tool for remote tracking of volcanic activity. *EOS Trans Am Geophys Union* 84(40):409–424
- Houghton BF, Swanson DA, Rausch J, Fagents SA (2008) Tephra dispersal during explosive events of the 2008 eruption of Halema'uma'u Crater, Kīlauea, Eos Trans Am Geophys Union 89(53) Fall Meet Suppl Abs V51E-2092
- James MR, Lane SJ, Chouet B, Gilbert JS (2004) Pressure changes associated with the ascent and bursting of gas slugs in liquid-filled vertical and inclined conduits. *J Volcanol Geotherm Res* 129:61–82
- James MR, Lane SJ, Chouet BA (2006) Gas slug ascent through changes in conduit diameter: Laboratory insights into a volcano-seismic source process in low-viscosity magmas. *J Geophys Res* 111:B05201. doi:10.1029/2005JB003718
- Jaupart C, Vergnolle S (1988) Laboratory models of Hawaiian and Strombolian eruptions. *Nature* 331:58–60
- Jaupart C, Vergnolle S (1989) The generation and collapse of foam layer at the roof of a basaltic magma chamber. *J Fluid Mechanics* 203:347–380
- Johnson JB, Harris AJL, Hoblitt RO (2005) Thermal observations of gas pistonning at Kīlauea Volcano. *J Geophys Res* 110:B11201. doi:10.1029/2005JB003944
- Landi P, Marchetti E, La Felice S, Ripepe M, Rosi M (2011) Integrated petrochemical and geophysical data reveals thermal distribution of the feeding conduits at Stromboli volcano, Italy. *Geophys Res Lett* 38:L08305. doi:10.1029/2010GL046296
- Lautze N, Harris AJL, Bailey JE, Ripepe M, Calvari S, Dehn J, Rowland SK, Evans-Jones K (2004) Pulsed lava effusion at Mount Etna during 2001. *J Volcanol Geotherm Res* 137:231–246
- Manga M (1996) Wave of bubbles in basaltic magmas and lavas. *J Geophys Res* 101:17,457–17,465
- Menand T, Raw A, Woods AW (2003) Thermal inertia and reversing buoyancy in flow in porous media. *Geophys Res Lett* 30(6):1291. doi:10.1029/2002GL016294
- Mudde RF (2005) Gravity-driven bubbly flows. *Annu Rev Fluid Mech* 37:393–423
- Navon O, Lyakhovskiy V (1998) Vesiculation processes in silicic magmas. In: Gilbert J S, Sparks RSJ (eds) *The Physics of Explosive Volcanic Eruptions*. *Geol Soc Lon Sp Publ* 145:27–50
- Neri M, Acocella V (2006) The 2004–2005 Etna eruption: Implications for flank deformation and structural behaviour of the volcano. *J Volcanol Geotherm Res* 158:195–206
- Neri M, Behncke B, Burton M, Galli G, Giammanco S, Pecora E, Privitera E, Reitano D (2006) Continuous soil radon monitoring during the July 2006 Etna eruption. *Geophys Res Lett* 33:L24316. doi:10.1029/2006GL028394
- Noguchi K, Kamiya H (1963) Prediction of volcanic eruption by measuring the chemical composition and amount of gases. *Bull Volcanol* 26:367–378
- Oppenheimer C, Francis P, Burton M, Maciejewski AJH, Boardman L (1998) Remote measurement of volcanic gases by Fourier transform infrared spectroscopy. *Appl Phys B* 67:505–515
- Oppenheimer C, McGonigle AJS, Allard P, Wooster MJ, Tsanev V (2004) Sulfur, heat, and magma budget of Erta 'Ale lava lake, Ethiopia. *Geology* 32(6):509–512
- Oppenheimer C, Lomakina A, Kyle PR, Kingsbury NG, Boichu M (2009) Pulsatory magma supply to Erebus lava lake, Antarctica. *Earth Planet Sci Lett* 284:392–398
- Palma JL, Calder ES, Basualdo D, Blake S, Rothery DA (2008) Correlations between SO₂ flux, seismicity, and outgassing activity at the open vent of Villarrica volcano, Chile. *J Geophys Res* 113: B10201. doi:10.1029/2008JB005577
- Parfitt E (2004) A discussion of the mechanisms of explosive basaltic eruptions. *J Volcanol Geotherm Res* 134:77–107
- Patanè D, Mattia M, Di Grazia G, Cannavò F, Giampiccolo E, Musumeci C, Montalto P, Boschi E (2007) Insights into the dynamic processes of the 2007 Stromboli eruption and possible meteorological influences on the magmatic system. *Geophys Res Lett* 34:L22309. doi:10.1029/2007GL031730
- Patrick MR (2007a) The gas content and buoyancy of strombolian ash plumes. *J Volcanol Geotherm Res* 166:1–6
- Patrick MR (2007b) Dynamics of strombolian ash plumes from thermal video: Motion, morphology, and air entrainment. *J Geophys Res* 112:B06202. doi:10.1029/2006JB004387
- Patrick MR, Harris AJL, Ripepe M, Dehn J, Rothery DA, Calvari S (2007) Strombolian explosive styles and source conditions: insights from thermal (FLIR) video. *Bull Volcanol* 69(7):769–784
- Patrick M, Wilson D, Fee D, Orr T, Swanson D, Sutton J, Elias T (2008) Gas-pistonning associated with the 2008 summit eruption of Kīlauea Volcano, Hawai'i. *Am Geophys Union Fall Meeting Abs* V51E-2082
- Patrick MR, Orr TR, Wilson D, Sutton AJ, Elias T, Fee D, Nadeau PA (2010) Evidence for gas accumulation beneath the surface crust driving cyclic rise and fall of the lava surface at Halema'uma'u, Kīlauea Volcano. Abstract V21C-2339 presented at 2010 Fall Meeting, AGU, San Francisco, Calif, 13–17 Dec
- Patrick MR, Orr T, Wilson D (2011) Cyclic spattering, seismic tremor, and surface fluctuation within a perched lava channel. Kīlauea Volcano *Bull Volcanol*. doi:10.1007/s00445-010-0431-2
- Platt U, Stutz J (2008) *Differential Optical Absorption Spectroscopy Principles and Applications*. *Physics of Earth and Space Environments Series* Springer, Series
- Poland MP, Sutton AJ, Gerlach TM (2009) Magma degassing triggered by static decompression at Kīlauea Volcano, Hawai'i. *Geophys Res Lett* 36:L16306. doi:10.1029/2009GL039214
- Realmuto VJ, Abrams MJ, Buongiorno MF, Pieri DC (1994) The use of multispectral thermal infrared mapping of sulphur dioxide plumes: a case study from Mount Etna, Sicily, July 29, 1986. *J Geophys Res* 99:481–488
- Ripepe M, Gordeev E (1999) Gas bubble dynamics model for shallow volcanic tremor at Stromboli. *J Geophys Res* 104(B5):10,639–10,654
- Ripepe M, Rossi M, Saccorotti G (1993) Image processing of explosive activity at Stromboli. *J Volcanol Geotherm Res* 54:335–351
- Ripepe M, Poggi P, Braun T, Gordeev E (1996) Infrasonic waves and volcanic tremor at Stromboli. *Geophys Res Lett* 23(2):181–184
- Ripepe M, Ciliberto S, Della Schiava M (2001) Time constraints for modeling source dynamics of volcanic explosions at Stromboli. *J Geophys Res* 106(B5):8713–8727
- Ripepe M, Harris AJL, Carniel R (2002) Thermal, seismic and infrasonic evidences of variable degassing rates at Stromboli volcano. *J Volcanol Geotherm Res* 118:285–297
- Ripepe M, Harris A, Marchetti E, Ulivieri G (2008) Dynamics of Strombolian Activity. In: Calvari S, Inguaggiato S, Puglisi G, Ripepe M, Rosi M (eds) *The Stromboli Volcano, An Integrated*

- Study of the 2002–2003 Eruption. Am. Geophys. Union Geophys Mono 182, pp 39–48
- Salerno GG, Burton MR, Oppenheimer C, Caltabiano T, Tsanev VI, Bruno N (2009) Novel retrieval of volcanic SO₂ abundance from ultraviolet spectra. *J Volcanol Geotherm Res* 181:141–153
- Spampinato L (2008) Thermal imaging of Halema'uma'u Crater (Kīlauea volcano, Hawai'i) using a hand-held thermal camera Hawai'i, 10–17 May 2008. Open File Report Istituto Nazionale di Geofisica e Vulcanologia sezione di Catania Prot Int N UVVG2008/121
- Spampinato L, Calvari S, Oppenheimer C, Lodato L (2008a) Shallow magma transport for the 2002–3 Mt. Etna eruption inferred from thermal infrared surveys. *J Volcanol Geotherm Res* 177:301–312
- Spampinato L, Oppenheimer C, Calvari S, Cannata A, Montalto P (2008b) Lava lake surface characterization by thermal imaging: Erta 'Ale volcano (Ethiopia). *Geochem Geophys Geosyst* 9(12): Q12008. doi:10.1029/2008GC002164
- Spampinato L, Calvari S, Oppenheimer C, Boschi E (2011) Volcano surveillance using infrared cameras. *Earth Sci Rev* 106:63–91
- Sparks RSJ (1978) The dynamics of bubble formation and growth in magmas: A review and analysis. *J Volcanol Geotherm Res* 3:1–37
- Spilliaert N, Métrich N, Allard P (2006) S-Cl-F degassing pattern of water-rich alkali basalt: modelling and relationship with eruption styles on Mount Etna volcano. *Earth Planet Sci Lett* 248:772–786
- Stoiber RE, Jepsen A (1973) Sulphur dioxide contributions to the atmosphere by volcanoes. *Science* 182:577–578
- Swanson DA, Duffield WA, Jackson DB, Peterson DW (1979) Chronological narrative of the 1969–71 Mauna Ulu eruption of Kīlauea Volcano, Hawai'i. US Geol Surv Prof Pap 1056:55
- Symonds RB, Mizutani Y, Brigs PH (1996) Long-term geochemical surveillance of fumaroles at Showa-Shinzan dome, Usu volcano, Japan. *J Volcanol Geotherm Res* 73:177–211
- Tilling RI (1987) Fluctuations in surface height of active lava lakes during 1972–1974 Mauna Ulu eruption, Kīlauea Volcano, Hawai'i. *J Geophys Res* 92:13,721–13,730
- Torrence C, Compo GP (1998) A practical guide to Wavelet Analysis. *Bull Am Met Soc* 79(1):61–78
- Varley NR, Taran Y (2003) Degassing processes of Popocatepetl and Volcán de Colima, Mexico. In: Oppenheimer C, Pyle DM, Barclay J (eds) Volcanic Degassing. Geol Soc Lon Spec Pub 213 Geol Soc Lon, pp 263–280
- Vergnolle S, Brandeis G (1996) Strombolian explosions: a large bubble breaking at the surface of a lava column as a source of sound. *J Geophys Res* 101:20,433–20,448
- Vergnolle S, Jaupart C (1986) Separate two-phase flow and basaltic eruptions. *J Geophys Res* 91:12,842–12,860
- Vergnolle S, Jaupart C (1990) Dynamics of degassing at Kīlauea volcano, Hawaii. *J Geophys Res* 95:2793–2809
- Vergnolle S, Mangan MT (2000) Hawaiian and Strombolian eruptions. In: Sigurdsson H, Houghton B, McNutt SR, Rymer H, Stix J (eds) Encyclopedia of Volcanoes. Academic, Academic Press San Diego, pp 447–461
- Vergnolle S, Ripepe M (2008) From Strombolian explosions to fire fountains at Etna Volcano (Italy): what do we learn from acoustic measurements? *Geol Soc Lond Sp Pap* 307:103–124
- Wilson L (1980) Relationship between pressure, volatile content and ejecta velocity in three types of volcanic explosion. *J Volcanol Geotherm Res* 8:297–313
- Wilson D, Elias T, Orr T, Patrick M, Sutton J, Swanson D (2008) Small explosion from new vent at Kīlauea's summit. *Eos Trans Am Geophys Union* 89:203
- Xu JL, Cheng P, Zhao TS (1999) Gas–liquid two-phase flow regimes in rectangular channels with mini/micro gaps. *Int J Multiphase Flow* 25:411–432